CHAPTER 2

BAINITIC STEEL

2.1 Introduction

Bainitic in steel has been defined[ASM, 1985] as "a eutectoid transformation product with a fine dispersion of carbide generally formed below 450-500°C". This limited expression describes only the classical forms of bainitic steel, there are also carbide free bainitic steels. A fuller description is given in the same reference by Edmonds[1985] - "bainite is the microstructure resulting from the decomposition of austenite in steels at temperatures above the martensitic transformation and below the pearlite reaction. In plain carbon steels, however, the bainitic temperature range overlaps the pearlite reaction range considerably. In many alloy steels the bainitic range is separate from the pearlite reaction range. The transformation can occur isothermally or during continuous cooling". Continuous cooling over a range of cooling rates, as found with thick sections, produces a range of bainitic structures.

In some non-ferrous alloys, transformation products form with a similar morphology to classical bainitic steel and these are known as bainites, but this does not infer a similar transformation mechanism. Only bainitic steel will be discussed in this work.

Unlike the other two common time-temperature steel transformation products, pearlite and martensite, the precise transformation mechanism of the bainitic reaction is still not fully understood and has been the subject of many (heated) debates. This is discussed in Section 2.3.

2.2 Bainitic structures

Classical forms of bainitic steel have been termed "upper" and "lower" bainite with reference to the respective transformation temperature ranges. Other common notations used at present for these structures are "BII bainite" and "BIII bainite" respectively. Such structures usually develop in medium and high carbon steels.

BII (upper) bainite

This structure is normally formed by transformations between 350 and 650°C. This structure consists of an aggregate of ferrite "laths" or "plates", grouped in "packets", with carbide precipitated along lath boundaries and at lath tips. During transformation the carbon content of the austenite increases so that the ferrite formed has little carbon left in solution.

BIII (lower) bainite

This structure consists of an aggregate of finer laths or plates with carbide precipitated predominantly within laths and at a distinct orientation (55 - 60°) to a lath axis; lath tips are free of carbide. Lower bainite is usually formed by transformations between 350°C and the M_s temperature. A considerable amount of carbon remains in solution within the ferrite matrix.

In a study of low carbon, low alloy steels, Irvine and Pickering[1957] noted that these steels could exhibit high strength and toughness when transformed over a range of cooling rates. For most section sizes, such steels continously cool to form bainitic structures. An example of a CCT diagram for such a steel, after Habraken and Economopoulos[1967], is given in Figure 2.1. (The effect of adding a small amount of boron to such a molybdenum steel is to retard the ferrite-pearlite transformation and thus increase the range of continuous cooling rates for bainitic transformations. Titanium and aluminium additions restrict boron oxidation.) If continuously cooled rather than isothermally cooled, many low carbon low alloy steels form bainitic structures which are predominantly free of carbide; most of the carbon is retained in solution. These steels are generally grouped under two broad descriptions; carbide-free, acicular bainite, often referred to as "BI bainite"[Habraken and Economopoulos, 1967; Ohmori et al, 1971] and "massive" or "granular" bainite, sometimes referred to as "BIV bainite"[Samuel et al, 1987].

BI bainite ("carbide free", acicular)

This structure consists mainly of highly dislocated, fine ferrite laths. In some structures no secondary phases are present; in others, secondary phases are present

in one of the following ways:

* Small amounts of acicular martensite within ferrite laths.
* Fine particles of either martensite or mixed martensite-austenite ("MA") phase between ferrite laths.
* Large areas of MA phase between ferrite laths resulting in a pseudo-lamellar structure[Harbraken and Economopoulos, 1967].

BIV bainite (granular, massive)

There appears to be no agreed precise description of this form of bainite. Examining low alloy steels with less than 0.3wt% carbon, Habraken and Economopoulos[1967] describe as "granular" a structure where much of the ferrite is granular in aspect, and as "massive", a structure consisting of coarse ferrite plates. Their experimentation produced a mix of such structures. In some of these, a degree of acicularity of large plates was observed. In such BIV bainites, distinct areas of MA phase are located along prior austenite grain boundaries (but rarely continuously) and also within prior austenite grains (along plate boundaries where applicable). At slower cooling rates, dependent upon alloy composition, some areas of MA phase partially decompose to ferrite and carbide; such carbide can be similar to upper bainitic carbide in appearance. Habraken and Economopoulos[1967] clearly show that MA phase areas consist of a central region of martensite bordered by retained austenite. In some structures, thin laths of martensite are visually discernible (by scanning electron microscopy) within MA phase areas, and occasionally, carbide precipitates or twins are found within these laths.

Other descriptions of a characteristic microstructure, resulting from a massive type transformation, state that grain boundaries mainly consist of a series of indented straight segments but with some curved boundaries (i.e. of the polygonal type[Massalski, 1987; Plichta, 1987]). Lui et al[1987] describe as "granular ferrite", a structure which consists of coarse plates of ferrite with/or areas of ferrite which are granular in aspect. Both forms of ferrite have a high dislocation density. Callender[1983] describes "granular bainite" as a heavily dislocated, lath free "massive" ferrite matrix, containing islands of MA phase. The martensite within these islands is twinned, indicating that it has a

carbon content in excess of 0.4wt%. The retained austenite is located both around the outside of the islands and it also between martensite plates. MA phase forms discontinuously along prior austenite grain boundaries, making them readily visible to microscopy. Bulloch[1988] describes a granular structure as acicular with islands of martensite, whereas Samuel et al[1987] describe a granular structure as one containing massive areas of ferrite in the neighbourhood of granules of bainite. Reynolds and Aaronson[1987] describe granular structures in Fe-C-Mo alloy steels as consisting of coarse aggregates of $(Fe,Mo)_3C$ and ferrite. Clayton et al[1987] and Callender[1983] describe BIV bainite as "lath-free", however Habraken and Economopoulos[1967] show that some acicularity can exist.

In this text, the Habraken and Economopoulos[1967] interpretation of a "BIV bainite", as one containing mixed "massive" and "granular" forms of ferrite plus a distribution of MA phase, will be used. Their schematic interpretation of the cooling routes required to form the different bainitic structures in low carbon alloy steels is shown in Figure 2.2 and that of Callender[1983], for low carbon, low alloy steels, is shown in Figure 2.3. A schematic representation of the different austenitic transformation products, and the different bainitic structures, is shown in Figure 2.4. The mix of bainitic structures within a relevant steel alloy will be dependent upon its composition, the cooling rate and any thermomechanical treatment before, or during, transformation.

2.3 Austenite to bainite displacive transformations

At slow cooling rates, the equilibrium transformation of eutectoid austenite to pearlite is controlled by the diffusion of carbon ahead of a glissile (moving) transformation interface. In austenite, carbon is fully in solution with its atoms in interstitial sites within the face-centred cubic (FCC) lattice. With equilibrium transformation, most of the carbon comes out of solution and cementite lamellae form, together with body centred cubic (BCC) ferrite.

At rapid cooling rates, the non-equibrium transformation of austenite to martensite is controlled by the near-instantaneous 'shear re-alignment' of the austenite lattice into

a body centred tetragonal (BCT) lattice where carbon is retained in solution; ie, a high energy, non-equilibrium, diffusionless, displacive transformation. For steels, this transformation involves a shape change as BCT unit cells form from FCC unit cells. This results in an directional increase in unit cell volume. Subsequently martensite plates are lens shaped in order to accommodate lattice strain.

Transformations from austenite to the various bainitic structures occur over a range of cooling conditions between those required for the pearlite and martensite transformations. BI, BII, BIII bainites, and some components of BIV bainite, transform by a displacive type reaction. (The transformation of BIV bainite is discussed in Section 2.4.) The martensite reaction is temperature dependent (athermal); if held isothermally, the transformation interface can be frozen [Reed-Hill, 1967], however bainite transformations are time dependent, as is the pearlite reaction. If held isothermally, most bainite reactions continue but do not go to completion between the B_s and B_f temperatures; thus implying a temperature dependency between definitive start and finish temperatures as seen in the martensite reaction (M_s and M_f). Like pearlite, BII (upper) and BIII (lower) bainites are a mixture of ferrite and carbide, but unlike pearlite, the composition of bainitic ferrite and carbide, with respect to substitutional alloying elements, remains the same. Pearlite grows in the form of spheres or nodules. BI, BII and BIII bainites and some BIV bainites grow as plates, a feature typical of martensite transformations. However martensite plates form within a fraction of a second whereas bainite plates grow "slowly" and continuously. In many alloys, the bainite transformation results in surface distortions, another feature typical of the martensite (lattice shear) reaction. Simplistically, the question is whether the bainitic transformation is controlled by carbon diffusion, by a diffusionless, "shear-type" transformation or by a mixture of both mechanisms. This issue is still a subject of intense academic debate.

Bhadeshia[1987] proposed that BI, BII and BIII bainitic ferrite do not form by a diffusional transformation mechanism, but by a sessile, displacive reaction. During the nucleation of aggregates of carbide platelets, carbon rapidly diffuses into residual austenite until its level of concentration is such that it prevents any further

diffusionless transformation; hence the incomplete reaction phenomenon. Transformation interface growth rates at the start of the bainite reaction far exceed calculated rates for growth controlled by carbon diffusion. This explains why bainite plates are restricted in their growth by austenite grain boundaries. After nucleation, new platelets form on those already present. Therefore bainite plates form by a martensite type lattice shear reaction *but* one where there is a redistribution of carbon and where nucleation is generally limited to austenite grain boundaries. The transformation interface (plate length) is eventually stopped by accumulating dislocation "debris" during growth, and plate width growth by hard impingement against other plates, i.e. sheaves develop which consist of clusters of fine platelets. Bhadeshia's summary of transformations from austenite in steels is shown in Table 2.1 and Figure 2.5. These do not separately distinguish "massive" ferrite from ferrite where there is no plate morphology. To summarise, in BII (upper) and BIV (granular) bainites, once the ferritic component of bainite has begun to form, the remaining areas of austenite are progressively enriched in carbon. These transform to ferrite and carbide in conventional upper (BII) and lower (BIII) bainites or partially to martensite in acicular (BI) and massive (BIV) bainites. With more rapid cooling, BIII (lower) and BI (acicular) bainites transform with large amounts of carbon retained in solution within the ferrite, despite its low solubility.

Aaronson and Reynolds[1987] have studied bainitic type transformations in several metal systems (eg. Ti-Cr) including steels. They proposed that the nucleation and growth of bainite are diffusion controlled mechanisms and that bainitic growth occurs in the form of ledges, as with pearlite, although there are fundamental differences between the two mechanisms. Phases of pearlite grow together via shared ledges, whereas the constituent phases of bainite grow along independent ledge systems. They maintain that the incomplete reaction phenomenom is erroneous and that some Fe-C-X alloys transform completely to bainite. They make a case that some diffusion controlled growth processes can exhibit invariant plane strain relief effects, typical of "shear-type" transformations, and that this results from the special effects of certain alloying elements upon the mechanism and from the kinetics of ferrite formation in steel. It is only within these certain alloys (including Fe-C-Mo alloys) that the overall

reaction kinetics definition of bainite (presumably Bhadeshia's work) has any validity.

Oblak and Hehemann[1967] studied the growth and structure of Widmanstatten ferrite and bainite in Fe-C-Mn-Si steels, some alloyed with Cr, Mo and Ni. By comparative usage of optical and electron micrographs they dismissed diffusion controlled growth as a mechanism for bainite formation in these steels. They propose that both BII (upper) and BIII (lower) bainite form by a far quicker mechanism, where sub-structural units rapidly propagate to a limiting size; i.e. the growth rates measured on a hot stage microscope were determined by the nucleation rates of these units. The rate at which carbon precipitates from the super-saturated baintic ferrite being formed determines the resultant type of bainitic structure (where the alloy forms conventional BII and BIII type bainites). Fast cooling rates result in rapid precipitation of ε-carbide in BIII (lower) bainite; this inhibits significant carbon enrichment of the remaining austenite. With BII (upper) bainite, slower cooling rates allow carbon enrichment of austenite trapped between advancing ferrite laths. Cementite usually precipitates from this enriched austenite, although its presence is not required as a criterion for defining bainite (as with BI and BIV bainites).

Olson, Bhadeshia and Cohen [1987] proposed a theoretical model involving both the "shear" and "diffusion" types of transformation, for crystalline phases containing both substitutional and interstitial elements. As a possible model for bainitic transformations, calculations for plate lengthening velocity for the mixed interface and diffusion controlled displacive transformation of an Fe-0.4wt%C alloy were given. The austenite to ferrite transformation process for alloy steels has been termed "para-equilibrium" by the authors; this is where the substitutional lattice may be considered "frozen" across the transformation interface, but where there is a redistribution of carbon interstitial atoms to achieve equality of chemical potential in both phases. In this process, growth is controlled by the diffusion of carbon in austenite ahead of the interface. A transformation where all the solute atoms are "frozen", as in the martensite reaction, is a "non-equilibrium". A more general case of non-equilibrium transformation is where none of the elements achieve equality of

chemical potential *but* where, unlike the martensite reaction, there is some redistribution of interstitial solute atoms, i.e. the ferrite grows with a partial supersaturation of carbon.

These authors considered the energy requirements for the nucleation and growth of a martensite type "shear" displacive transformation interface, whilst there is carbon redistribution across that interface.The free energy considerations, with respect to the velocity of a displacive transformation interface, indicated that some (carbon) solute redistribution would allow a displacive transformation to start above the M_s temperature. From these calculations, the degree of carbon supersaturation in ferrite, with respect to transformation temperature, is shown in Figure 2.6 and the respective isothermal transformation diagram in Figure 2.7. In Figure 2.6, the temperature at which supersaturation becomes <0.5 was suggested (by the authors) as a possible transition point for BII (upper) to BIII (lower) bainite, denoted by "L-U". This model predicts that the time during nucleation is much larger than during initial growth, so that the size distribution of bainite platelets will include a distribution of very fine platelets, which are below the critical size required for rapid growth. Such a feature is indicated on TEM micrographs. To summarise, this model predicted an increasing transformation interfacial velocity and carbon supersaturation in ferrite during growth with decreasing transformation temperature, while the nucleation velocity passes through a maximum (ie, "C-curve kinetics"). The nuclei become fully supersaturated at the M_s temperature.

2.4 Austenite to BIV (massive or granular) bainite

With non-equilibrium continuous cooling, there can be a rapid transformation from austenite to another phase, with no substitutional alloy redistribution. If there is also no carbon redistribution, b.c.t. martensite is formed. If there is high carbon supersaturation, but with some precipitation out in the form of intra-lath carbides, BIII (lower) bainite forms. If the cooling rate is such that carbon has time to diffuse into the residual austenite, BII (upper) bainite forms, with inter-lath carbide. If the carbon content is low and the cooling rate initially slow, carbide free structures form (Figures 2.2 and 2.4) by either a displacive reaction, resulting in laths with intra or

inter-lath martensite or MA phase (as in BI bainite), or, at a slower initial cooling rate, a massive type transformation to form BIV granular bainite. With this type of transformation, the limited carbon diffusion makes more of a contribution to the control of nucleation and growth, resulting in a structure of ferrite grains with mixed straight and curved boundaries. (This could be schematically viewed as a mix of plate and polygonal morphologies.) The enriched austenite partially transforms to form MA phase at both plate and grain boundaries. Prior austenite grain boundaries are preferred nucleation sites. With a plate structure these boundaries will remain.

In a review of massive transformations, Massalski[1985] stated that the transfer of atoms across the transformation interface is not fully understood; it does not appear to be a displacive "shear" type of transformation. Transformation kinetics are controlled by interface diffusion and other interface variables such as coherence; growth occurs by displacement of incoherent (high energy) boundaries. There are no simple lattice orientation relationships between the parent and product phases. In Table 2.1, Bhadeshia[1987] classed massive transformations with that of allotriomorphic ferrite (though with many "inconsistent" signs against certain features). Plichta[1987] has studied massive transformations in several metallic alloy systems, including iron. Such transformations are based upon, (a) thermodynamics, where a favourable allotropic type transformation is present within the phase diagram and (b) kinetics, where diffusional processes are at such a rate that this form of transformation is favoured against others.

In proposing a tentative mechanism for transformation to BIV (granular) bainite, Habraken and Economopoulos[1967] pre-supposed that there is a degree of dehomogenization of carbon within austenite, prior to transformation. Carbon depleted areas then transform by a process similar to that of massive martensite in carbon-free ferrous alloys. A degree of diffusion would enrich residual austenite areas in carbon (Figure 2.2, cooling route III). Thermodynamic conditions near, or within, these carbon rich areas are not adequate for carbide nucleation, therefore MA phase forms. Transformation is often nucleated from austenite grain boundaries, this results in a structure similar to BII (upper) bainite if there is a plate morphology,

but with MA phase instead of carbide. At a faster initial cooling rate, there would be a more acicular structure and a finer distribution of carbon rich, residual austenite. Dependant upon the steel composition, this would give BI (carbide free, acicular) bainite or BIII (upper) bainite (Figure 2.2, cooling route II).

Callender[1983] has reviewed the transformation theory of austenite to BIV granular bainite. He places the discussion in two catagories:

A massive transformation. The mechanism as decribed by Habraken and Economopoulos [1967] above. Ferrite is thought to nucleate primarily at some areas along prior austenite grain boundaries, although MA phase exists discontinuously along these boundaries as well as within prior austenite grains. A study of micrographs of this BIV bainite indicated that this is possible with the directional nature of the transformation interface within a prior austenite grain, as within other "blocky" structures such as BII (upper) bainite. With an increase in cooling rate, increase in carbon content or decrease in transformation temperature, massive type transformations are suppressed and displacive "shear" type transformations are favoured. Therefore, with continuous cooling, mixed massive / lath microstructures can readily exist within the same prior austenite grain.

BIV (granular) bainite as degenerate BII (upper) bainite. It has been proposed by some authors that pertubations in the sides of upper bainitic laths "bridge" across to other laths thus trapping areas of residual austenite, which are subsequently enriched in carbon. Callender showed that such a mechanism is unlikely.

2.5 Strengthening mechanisms for bainitic steels.

Dislocation density

One strengthening mechanism is that the structure can hold a high dislocation density, in addition to retained austenite, when compared to polygonal ferrite. These dislocations are generated by the rapid displacive nature of the transformation and the strength of the structure is related to the average dislocation density (i.e. UTS $\propto$ $\sqrt{(\text{dislocation density})}$[Callender, 1983]). Oblak and Hehemann[1967] found that a significant

difference between Widmanstatten ferrite and BII (upper) bainite was the latter's higher dislocation density. In BIII (lower) bainite, super-saturation of carbon, and the resultant precipitaion of fine carbides within laths, generates a high density of dislocations; far higher than in BII (upper) bainite.

Dispersion and volume fraction of hard phases

Irvine and Pickering[1957] found that the tensile strength of conventional BII and BIII bainites was dependent on carbide distribution and grain size. The finer the carbide dispersion, both within and between laths, the higher the material strength. With respect to each alloy, the lower the transformation temperature, the finer the carbide dispersion. In low carbon alloys, where carbides are present, reduction in grain size is the primary method for hardening due to the low volume fraction of carbide.

In low carbon, low alloy (BI and BIV) bainitic structures, MA phase is the dominant hard phase rather than carbide. The average hardness of this phase is thought to be around 500 HV[Bush and Kelly, 1971]. There is a hardness gradient across a MA phase region as they usually consist of martensite bordered by retained austenite. This was clearly illustrated by Habraken and Economopoulos[1967]. Cementite and other iron carbides have hardness values of 1000 to 1500 HV.

Bush and Kelly[1971] found that in carbide free, BI and BIV bainites, second phase hardening from MA phase was dependent upon the strength and volume fraction of that phase. The strength of MA phase is dependent upon its carbon content (i.e. upon the cooling curve for a given alloy). Bulloch[1988] found that tensile and yield strengths were linearly related to volume fraction of MA phase (up to 70%) and that increasing this volume fraction increased the minimum stress range, below which, short micro-cracks propagated (or coalesced), but it decreased the threshhold stress intensity range, below which, long microcracks ceased to propagate (i.e. ductility was reduced).

If MA areas become coarse, and particularly elongated, impact strength becomes greatly decreased whilst tensile strength and ductility are relatively unaffected. With

BI bainite, a high volume of acicular martensite in inter-lath locations results in a marked increase in tensile strength but reduced ductility[Callender, 1983].

Transformation temperature

Within the bainitic range of transformations, the lower the transformation temperature, the higher the dislocation density (with more carbon retained in solution) and the finer the dispersion of hard phases; i.e. the higher the material strength. For BII and BIII bainites, there is an inverse linear relationship between transformation temperature and tensile strength[Pickering, 1967] (Figure 2.8a). The lower the transformation temperature, the smaller the width of bainitic plates, although plate length will be determined by prior austenite grain size[Irvine and Pickering, 1957]. Steven and Haynes[1956] determined a relationship for low alloy, low carbon steels for the bainitic transformation start temperature (isothermally) where;

$$B_s \pm 25°C = 830 - 270(\%C) - 90(\%Mn) - 37(\%Ni) - 70(\%Cr) - 83(\%Mo)$$

and the B_s to B_f range = 120°C

Haynes[1966] further qualified this expression for continuous cooling by reducing the constant to 810°C and increasing the B_s to B_f range to 195°C.

Grain size

Ferritic bainite, in both plate/lath and granular form, nucleates and grows from austenite grain boundaries[Harbraken and Economopoulos, 1967]. Within those grain boundaries, the size of plate packets and the semi-straight segmented boundaries of granular bainite, will be determined by the transformation temperature; the lower the temperature the finer the size. The finer the overall structure, in terms of both grain size and packet size, the higher the strength (UTS $\propto 1/\sqrt{\{\text{grain size}\}}$)[Pickering, 1967]. For a given transformation temperature, the lath "packet" size is specifically determined by prior austenite grain size (Figure 2.4); the finer this grain size, the higher the yield stress[Callender, 1983].

Internal stress

The displacive type transformation of austenite to plate/lath bainitic ferrite results in lattice strain, particularly with BIII (lower) bainite. This is generated by the volume change resulting from austenite f.c.c. unit cells changing to ferrite b.c.c. unit cells. Such internal stress slightly increases material strength but reduces the 0.2% proof stress / ultimate tensile strength (PS:UTS) ratio. In BI (carbide free, acicular) bainite, if any acicular martensite forms within bainitic laths, there is a marked increase in tensile strength, together with a marked decrease in impact resistance[Harbraken and Economopoulos, 1967].

Interstitial solid solution strengthening

Many authors have determined that the strength increase due to this mechanism is proportional to $\sqrt{(C+N)}$ in both bainite and martensite, by both interstitial solid solution hardening and dislocation interaction[e.g. Callender 1983]. This effect will be particularly marked with lower bainite but far more so within a martensitic structure.

Substitutional solid solution strengthening

The strength of steels air-cooled to form conventional BII (upper) and BIII (lower) bainites can be predicted from their chemical composition. For steels with up to 0.25 wt% carbon, Steven and Haynes[1956] gave this relationship (wt.% of elements are given):

$$\text{UTS (tsi)} = 16 + 125C + 15(Mn+Cr) + 12Mo + 6W + 8Ni + 4Cu + 25(V+Ti)$$

Pickering[1967] confirmed the validity of this relationship. With respect to cooling characteristics, nickel stabilises austenite thereby lowering transition temperatures and increasing bainitic hardenability, (i.e. in low carbon steels, the incidence of lower bainite). Alloying additions should be such that the M_s and B_s temperatures are not too close, so as to minimise any martensite reaction during continuous cooling.

The effect of boron

Small quantites of boron have a marked effect on the cooling transformation characteristics of certain steels, particularly low alloy 0.5% molybdenum steels, by extending the range of cooling rates over which bainitic structures will form. This has been schematically illustrated by Pickering[1967] (Figure 2.8b). Hume-Rothery[1966] relates this behaviour to the atomic diameter of boron. Its size is such that it fits neither interstitial nor substitutional sites and is hence attracted to lattice irregularities, such as grain boundaries and dislocations, thus relieving local strain fields and stabilising austenite. The effect is to retard the formation of pro-eutectoid ferrite and upper bainite. Callender's survey[1983] found that boron was only effective in combination with molybdenum or tungsten in increasing hardenability and reducing the B_s temperature. Aluminium, titanium and zirconium traces must be added to prevent boron oxidation or nitridation. To prevent coarse $Fe_{23}(C,B)_6$ precipitates forming, higher austenitizing temperatures are required. The effectiveness of boron (in solution) is optimum at ≤ 0.002 wt.%, this being thought sufficient to fill lattice irregularities[Hume-Rothery, 1966]. If the content exceeds this, strain is re-introduced into the lattice and the effect negated. The effect lessens with increasing carbon content and it does not affect the formation of pearlite.

Inclusions

Any brittle non-metallic inclusions can crack under stress thereby initiating, or facilitating, cleavage propagation. This reduces impact properties and fracture toughness. Ductile manganese sulphide inclusions, often associated with shrinkage voids[Brooksbank and Andrews, 1970], can adversely affect impact properties by reducing upper shelf energy, though not lower shelf energy. The presence of inclusions, brittle or ductile, lowers fatigue stength.

2.6 Mechanical properties

As discussed above, tensile strength is inversely linearly proportional to transformation temperature and directly related to sustitutional alloy composition. The tensile strength appears to be insensitive to continuous cooling rates (a valuable asset for weldability). 0.2% PS:UTS ratios are in the range of 0.7 to 0.8 over a

wide range of compositions for conventional BII and BIII bainites, but this ratio is reduced to around 0.6 if MA phase is present (BI and BIV bainites)[Irvine and Pickering, 1957]. These authors restored the ratio by low temperature tempering one structure; there was no apparent change in this microstructure. This indicates that residual stresses are associated with the presence of MA phase.

For both BII (upper) and BIII (lower) bainites, ductility increases as the transformation temperature increases (i.e. as dislocation density and carbide dispersion decrease), however their comparative impact properties follow the pattern shown in Figure 2.9. This clearly shows that lower bainites have a comparatively better impact resistance than upper bainites as well as superior tensile strength. Pickering [1967] relates this to the pattern of carbide dispersion. The location of carbide in a BII upper bainitic structure, at grain boundaries and between the laths, does not present an effective barrier to the propagation of cleavage cracks. Cleavage cracks only deviate at boundaries between lath packets or prior austenite grain boundaries. Callender[1983] found that these are high angle, high energy boundaries and that impact resistance was closely related to lath packet size and the related prior austenite grain boundary size in upper bainites. There are also high energy boundaries between sub-units within a lath. At the expense of tensile strength the impact properties can be recovered to a degree by tempering upper bainites (thus reducing grain boundary energy and dislocation density), except for low carbon steels where the ferrite grain boundary energy is low enough to resist tempering. In BIII (lower) bainitic structures, fine carbide precipitation within laths, the absence of inter-lath carbide and the small lath packet size all contribute to low cleavage crack propagation rates and hence, high ductility.

Callender [1983] found some correlation between (Charpy) impact properties and fracture toughness, but this was limited with some marked deviations. Transition temperatures for impact tests were higher due to higher strain rates.

Under fatigue testing, all four types of bainitic steel structures form dislocation cells, i.e. areas of low dislocation density bordered by areas of high dislocation

density[Callender, 1983]. Some can span a complete lath thus forming a rectangular cell. During testing there is initial strain hardening and then cyclic softening as these cells form. MA areas are incorporated into cell walls thus reducing overall boundary energy. At low cyclic strain amplitudes, dislocation cell formation only occurs in BIV (granular) structures, i.e. this type of structure has comparatively lower fatigue resistance.

Bhadeshia[1992] has commented on the differences in mechanical properties between carbide containing bainites (upper and lower) and carbide-free bainites (with MA phase). He attributed the inferior toughness of carbide containing bainites to void nucleation and cleavage on carbide particles. Additionally, carbide-free bainites have less carbon in solution in bainitic ferrite thus further increasing toughness and also, within MA phase areas, stress induced transformation of austenite to martensite would restrict crack propagation. However, if MA phase areas are too blocky, the (stress induced) formation of large areas of untempered martensite would have an embrittling effect. For optimum toughness, MA phase should be distributed as a "film" between laths and plates.

2.7 Summary note on bainitic structures.

Alloy steel components, manufactured to primarily produce a bainitic structure, are continuously cooled at a rate such that the resultant structure usually consists of a mix of bainitic structures with, in some cases, areas of martensite and pearlite (Figures 2.2 and 2.3). Resultant mechanical properties will reflect this mix.

2.8 The bainitic steels used in this wear study

Choice of composition

Previous work on the dry wear behaviour of bainitic steels for railway line usage has been discussed in Chapter 1. With the exception of Callender's work[1983], at the time this work commenced there has not been a systematic approach linking wear properties to bainitic structures. Callender investigated bainitic structures with a view to their use as a rail crossing material, where the critical area of the crossing nose requires a high resistance to both impact wear and fatigue and where the material

should have good weldability. He recommended a low carbon, low alloy bainitic steel and subsequently similar steels have since been successfully utilised for this purpose. However when such steels have been installed as curved rail track, which is subject to highly stressed rolling-sliding wear, their wear performance has been disappointing. Conventional pearlitic steel rails, with inferior mechanical properties to these experimental bainitic steel rails, appeared to have a higher resistance to rolling-sliding wear[Allery, 1985]. Similar results have been found in other countries where one, or a few, bainitic rail compositions have been assesssed for rolling-sliding wear resistance, on track and/or in the laboratory[Heller and Schweitzer, 1982; Kalousek et al, 1985; Ichinose et al, 1978]. Yet low carbon, low alloy bainitic steels have shown good comparative wear properties to pearlitic rail steels in tests on a (pure sliding) pin on disc wear test rig[Clayton et al, 1987]. This is the most widely used form of wear test.

Wear resistance is often associated with overall material hardness and/or with the volume fraction and distribution of hard phases within a material. On this basis, three experimental, low alloy baintic compositions were chosen with variable carbon contents, but also with an alloy mix aimed at minimising differences in mechanical properties, i.e. by all the alloys having a common B_s temperature. This was to be achieved by varying the alloy composition in accordance with Stephen and Haynes formula for continuous cooling (see previous section on transformation temperature). The compositions used, and the theoretical B_s temperatures according to the formula, are given in Table 2.2, together with the compositions of the conventional pearlitic steel rail products used for comparative assessment. The bainites are notated as "B04, B20 and B52" (with respect to their carbon contents) throughout the present work. Averaged mechanical properties determined from several tests are given in Table 2.3; these are discussed later. Determinations of transformation temperature are given in Table 2.4. It can be seen from Table 2.4 that the cooling rates used for transformation temperature assessment resulted in material hardness values which differed from the bainitic barstock. However, the mechanical properties of these bainites, in comparison to the pearlitic steels, provided a good platform for the wear test programme.

Assessment of experimental bainitic barstock and pearlitic rail products.

The bainitic steels were cast and rolled at the British Steel Research Laboratories in Rotherham (Yorkshire, UK); B04 and B52 as 60mm diameter bar and B20 as 69mm diameter bar. Longitudinal and transverse sections were taken through the rolled lengths at several locations and examined by optical and (limited) electron microscopy. Samples from different parts of the rolled lengths were tested for nickel and chrome segregation (across the bar widths) and for mechanical properties (Table 2.3). The alloy compositions were also re-checked at different locations along and across the bars. These chemical analysis results were satisfactory. The pearlitic rail products were also checked for chemical composition (Table 2.2), mechanical properties (Table 2.3) and microstructure.

The structure of bainite B04.

Axial and transverse sections through the barstock had similar, homogenous structures; no banding was observed. The structure is shown in Figures 2.10 to 2.12. It is carbide free with inter-lath and non-continuous grain boundary areas of MA phase, within a coarse acicular (massive) structure. The acicularity is defined within the prior austenite grain boundaries. In carbide free bainites, there is no clear visual delineation between acicular BI and BIV bainitic structures; the continuous cooling regions are adjacent (Figure 2.3). This structure lies near that border area. Due to the "massive" nature of the acicularity the structure is best described as a BIV bainite. There are no matrix differences between transverse and longitudinal barstock microstructures, except for the directionality of a fine distribution of ductile MnS inclusions and occasional clusters of dark, opaque, brittle inclusions strung out in the rolling direction. These inclusions are thought to be metallic oxides and/or more brittle forms of MnS. There is also a fine distribution of angular, brittle TiN inclusions. These have no directionality. The inclusion content was low compared to the two pearlitic steels (note the comparative sulphur and phosphorus contents of the bainitic and pearlitic steels in Table 2.2).

The structure of bainite B20.

This structure is shown in Figures 2.13 to 2.15; it is free from carbide. There is a

high volume of inter-lath MA phase but, unlike B04, this phase does not delineate prior austenite grain boundaries. The volume of MA phase is such that it is difficult to assess the degree of acicularity within the structure; it appears to be less than in the B04 structure. There are some large curved grain boundaries (Figure 2.13a). This steel appears to be a BIV type bainite with a predominantly (massive) acicular structure. Some straight segments of matrix, typical of massive structures (as discussed by Habraken and Economopoulos [1967]), can be seen (Figures 2.13b and 2.14a). There is some directionality to the structure at the centre of the barstock (Figure 2.14b) but not toward the edge (Figure 2.14a). 47mm diameter disc wear test surfaces were situated around this latter location. Inclusion content and distribution are the same as B04. The density of MA phase is shown in the electron micrographs (Figures 2.15a & b).

The structure of bainite B52.

The general structure is shown in Figures 2.16 to 2.18. It consists of ferrite and carbide; there is no MA phase. The bulk of the matrix is BII (upper) bainite with inter-lath carbide (Figure 2.17a). There is also a considerable volume fraction of a lighter etching constituent within which there are distinct large laths. In this text these will be referred to as "large-lath" areas. The laths are large lenticular plates of BIII (lower) bainite within a matrix thought to be martensite. (Figures 2.17b and c). From the hardness (100 - 150 HV points higher than the general matrix) and rigidity of these regions (as observed in the wear induced, highly strained microstructures described in Chapter 9), it seems probable that this phase is auto-tempered martensite, rather than retained austenite, and that these "large lath" zones have a higher carbon content than the general matrix. An axial section of the B52 barstock examined at low magnification, indicated that the structure had a slight degree of directionality (Figures 2.18a and b), with bands of a more "acicular" general matrix. However, significant differences between transverse and longitudinal matrices are not readily apparent at higher magnifications. Inclusion content and distribution were the same as for B04 and B20. Typical inclusions in this bainite were short, ductile MnS "stringers" (Figure 2.16a), small, brittle Ti based inclusions and occasional small strings (in the rolling direction) of dark, opaque, brittle oxide inclusions.

Devanathan and Clayton[1991] also examined this material. They described the lighter etching areas as "twinned martensite" and made no mention of lower bainite. They found these areas slightly higher in Cr, Mn and Si. Their Knoop micro-hardness tests indicated that the martensite areas had a (Knoop) hardness of around 600 HK compared to 250 HK for the upper bainite regions.

The structures of the pearlitic rail products, BS11 rail and Type 'D' tyre.

Despite the small differences in composition, the two pearlitic structures are basically the same. The compositions are given in Table 2.2 and the mechanical properties in Table 2.3. (Type 'D' tyre properties are at the bottom end of the specified range for such a material, i.e. not quite typical.) Both products had been hot-worked and continuously cooled. The structures are shown in Figures 2.19 and 2.20. In both steels, there is a small volume fraction of pre-eutectoid "free" ferrite with a balance of conventional, pearlite, containing finely spaced carbide and ferrite lamellae. There are numerous MnS inclusions, elongated in the rolling direction. The MnS inclusion content is far higher, and the inclusions far coarser, than in any of the experimental bainitic structures. These inclusions are frequently located in areas of pro-eutectoid ferrite (Figure 2.20).

The mechanical properties of these bainitic and pearlitic steels.

Examples of (engineering) stress-strain curves for the different materials, used for the determination of mechanical properties (Table 2.3), are shown in Figure 2.21a. This shows that whereas B52 had a short period of strain from maximum loading to fracture, the two MA phase bainites, B04 and B20, had large periods of strain. This is also reflected in the true stress values for B04 and B20 compared with those of B52 (Table 2.3) and similarly with brittle/ductile transition temperature curves shown in Figure 2.21b. To summarise in value order, for UTS (engineering stress), B52 > B20 > B04; for true stress, B20 > B04 > B52 and for hardness, B20 > B52 > B04. In all aspects, the bainitic steels have superior mechanical properties to the pearlitic steels, except for the low ductility of B52. (Low ductility is a feature of upper bainitic structures, see Section 2.5.) The increased volume fraction of MA phase in B20, compared to B04, is reflected in their respective properties.

The differences between the mechanical properties of all five steels, particularly strain after maximum loading, are linked to phase boundary coherence. Carbide (pearlitic or bainitic) - ferrite boundaries have far less coherence and far more boundary energy than the MA phase - ferrite boundaries, therefore dislocation pile-ups and void formations (resulting in low ductility) will occur more readily at carbide boundaries [Bhadeshia and Edmonds, 1983]. Another major factor affecting this pattern of mechanical properties is the volume fraction, shape and dispersion of hard phases within the steels. This affects the "mean ferrite path", i.e. the ease with which dislocations can move between hard phases before dislocation pile-up, multiplication and subsequent hardening. Ferrite within all three bainitic structures will have a higher dislocation density than in the pearlite and pro- eutectoid ferrite structures of the rail steel products.

These mechanical properties are derived from *tensile* tests only. In the moving contact of curved surfaces, contacting areas are under a compressive stress from normal loading and cycles of compression and tension from rolling, or rolling-sliding. For example, whereas a crack may be generated at the high energy, low coherence boundary between carbide and ferrite in tension, this would not be the case in compression where stress would be absorbed by strain within ferrite areas. These factors are further considered in Chapter 9 (on "Examinations of worn discs").

2.9 Summary

Three bainites have been described whose mechanical properties have been explained in terms of their different microstructures. On this basis, their rolling-sliding wear behaviour has been critically examined and compared to that of established pearlitic rail steel.

Some of the results in this present work have been discussed in Bhadeshia's[1992] recent book "Bainite in Steels", in a section on the suitability of bainitic steels for railway applications.

2.10 References

Allery, M.B.P. {British Rail Research} (1985). Personal communication on the results of field trials where experimental bainitic rails have been laid in track curves amongst standard BS11 pearlitic rails.

ASM Metals Handbook 9th Edition (1985) 9, p.2 ("Definitions").

Bhadeshia, H.K.D.H. and Edmonds, D.V. (1983). "Bainite in steels: new composition - property approach, Parts 1 & 2." *Metal Science* 17 Sep. '83, pp. 411-425.

Bhadeshia, H.K.D.H. (1987). "Bainite in Steels." *Proc. Int. Conf. "Phase Transformations '87", 8-7-87, (Inst. of Metals), Univ. of Cambridge, UK.*

Bhadeshia, H.K.D.H. (1992). Bainite in Steels. Pub. Inst. of Materials.

British Standard 24 (1956). British Standards Institution.

British Standard 11 (1978). British Standards Institution.

British Standard 5892 (1986). British Standards Institution.

Brooksbank, D. and Andrews, K.W. (1970). "Stress fields around inclusions and their relation to mechanical properties." *Proc. Int. Conf. on "Production and application of clean steels", 23-26/6/70, Balantonfüred, Hungary.* Pub. Iron & Steel Inst. SR134 (1972) p.186.

Bulloch, J.H. (1988). "The fatigue limit characteristics of a range of granular bainitic microstructures." *Res. Mechanica* 23 pp. 1-12.

Bush, M.E. and Kelly, P.M. (1971). "Strengthening mechanisms in bainitic steels." *Acta Met.* 19 Dec. 1971, pp. 1363-1371.

Callender, W.R. (1983). "Bainitic steels for railway applications." *Ph.D. Thesis*, Univ. of Sheffield.

Clayton, P., Sawley, K.J., Bolton, P.J. and Pell, G.M. (1987). "Wear behaviour of bainitic steels." *Proc. Int. Conf. on "Wear of Materials", 5-9/4/87, Houston, Tex., USA.* Pub. *WEAR* 120 pp. 199-220.

Devanathan, R. and Clayton, P. (1991). "Rolling-sliding wear behaviour of bainitic steels." *WEAR* 151 (2), pp. 255-267.

Edmonds, D.V. (1985). ASM Metals Handbook 9th Edition 9, p.64.

Harbraken, L.J. and Economopoulos, M. (1967). "Bainitic microstructures in low carbon alloy steels and their mechanical properties." *Proc. Int. Symp. on "Transformation and Hardenability in Steels", 27-28/02/67, Univ. of Michigan.* Pub. Climax Molybdenum Co., Ann Arbor, Michigan.

Haynes, A.G. (1966). "Interrelation of isothermal and continuous cooling heat treatments of low alloy steels and their practical significance." *Heat treatment of Metals, I.S.I. SR95*, 13, ed. T.L. Hughes (Iron & Steel Institute, London).

Heller, W. and Schweitzer, R. (1982). "Hardness, microstructure and wear behaviour of rail steels." *Proc. 2nd. Int. Conf. on "Heavy Haul Railways", Colorado Springs, CO, 25-29/9/82*, pp. 282-286.

Hume-Rothery, W. (1966). The structures of alloys of iron, an elementary introduction, pp. 241-253. Perganon Press.

Ichinose, H., Takehara, J., Iwasaki, N. and Ueda, M. (1978). "An investigation on contact fatigue and wear resistance behaviour in rail steels." *Proc. 1st Int. Conf. on "Heavy Haul Railways", Perth, Australia, 18-22/9/78*. Austr. Inst. Engrs. & Austr. Inst. Mining & Metallurgy.

Irvine, K.J. and Pickering, F.B. (1957). "Low carbon bainitic steels." *J.Iron & Steel Inst.* (London) 187 pp. 292-309.

Kalousek, J., Fegredo, D.M. and Laufer, E.E. (1985). "The wear resistance and worn metallurgy of pearlite, bainite and tempered martensite rail steel microstructures of high hardness." *WEAR* 105 (3) pp. 199-222.

Lui, S.K., Cai, G. and Lui, L. (1987). "The granular bainite in V, Ti containing Fe-C alloys." *Proc. Int. Conf. "Phase Transformations '87", 8-7-87, (Inst. of Metals)*, Univ. of Cambridge, UK.

Massalski, T.B. (1985). "Massive transformation structures." ASM Metals Handbook 9th Edition 9, pp. 655-657.

Oblak, J.M. and Hehemann, R.F. (1967). "Structure and growth of widmanstätten ferrite and bainite." *Proc. Int. Symp. on "Transformation and Hardenability in Steels", 27-28/02/67, Univ. of Michigan*. Pub. Climax Molybdenum Co., Ann Arbor, Michigan.

Ohmori, Y., Ohtani, H. and Kunitake, T. (1971). "The bainite in low carbon low alloy high strength steels." *Trans. I.S.I. Jap.* 11 pp. 250-259.

Olson, G.B., Bhadeshia, H.K.D.H. and Cohen, M. (1987). "Coupled diffusionsal / displacive transformations." *Proc. Int. Conf. "Phase Transformations '87", 8-7-87, (Inst. of Metals)*, Univ. of Cambridge, UK. (Also pub. in *Acta Met* 37 (2), 1989, pp. 381-390.)

Pickering, F.B. (1967). "The structure and properties of bainite in steels." *Proc. Int. Symp. on "Transformation and Hardenability in Steels", 27-28/02/67, Univ. of Michigan.* Pub. Climax Molybdenum Co., Ann Arbor, Michigan.

Plitcha, M.R. (1987). "Massive transformations in various alloy systems." *Proc. Int. Conf. "Phase Transformations '87", 8-7-87, (Inst. of Metals)*, Univ. of Cambridge, UK.

Reed-Hill, R.E. (1967). Physical Metallurgy Principles. Pub. Van Nostrand.

Reynolds, W.T. and Aaronson, H.I. (1987). "Formation of granular bainite in Fe-C-Mo steels." *Proc. Int. Conf. "Phase Transformations '87", 8-7-87, (Inst. of Metals)*, Univ. of Cambridge, UK.

Samuel, F.H., Daniel, D. and Sudre, O. (1987). "Further investigations on the microstructure and mechanical behaviour of granular bainite in a high strength, low alloy steel: Comparison of ferrite-pearlite and ferrite-martensite microstructures." *Materials Science & Engineering* 92 pp. 43-62.

Stephen, W. and Haynes, A.G. (1956). *J.Iron and Steel Inst.* (London) 183 p.349.

The table below indicates the key characteristics of phase transformations in steels; it may be regarded as a working hypothesis which seems most consistent with the available experimental data. The nomenclature used for the transformation products is as follows: martensite (α'), lower bainite (α_{lb}), upper bainite (α_{ub}), acicular ferrite (α_a), Widmanstätten ferrite (α_w), allotriomorphic ferrite (α), idiomorphic ferrite (α_i), pearlite (P), substitutional alloying elements (X). Consistency of a comment with the transformation concerned is indicated by (=), inconsistency by ($\neq$); cases where the comment is only sometimes consistent with the transformation are indicated by ($\otimes$). The term *parent* γ implies the γ grain in which the product phase grows. Note that it is not justified to distinguish massive ferrite from α.

Table

Comment	α'	α_{lb}	α_{ub}	α_a	α_w	α	α_i	P
Nucleation and growth reaction	=	=	=	=	=	=	=	=
Plate morphology	=	=	=	=	=	≠	≠	≠
IPS shape change with shear component	=	=	=	=	=	≠	≠	≠
Diffusionless nucleation	=	≠	≠	≠	≠	≠	≠	≠
Only carbon diffuses during nucleation	≠	=	=	=	=	≠	≠	≠
Reconstructive diffusion during nucleation	≠	≠	≠	≠	≠	=	=	=
Often nucleates intragranularly on defects	=	≠	≠	=	≠	≠	=	≠
Diffusionless growth	=	=	=	=	≠	≠	≠	≠
Reconstructive diffusion during growth	≠	≠	≠	≠	≠	=	=	=
Atomic correspondence (all atoms) during growth	=	=	=	=	≠	≠	≠	≠
Atomic correspondence, during growth, for atoms in substitutional sites	=	=	=	=	=	≠	≠	≠
Bulk redistribution of X atoms during growth	≠	≠	≠	≠	≠	⊗	⊗	⊗
Local equilibrium at interface during growth	≠	≠	≠	≠	≠	⊗	⊗	⊗
Local paraequilibrium at interface during growth	≠	≠	≠	≠	=	⊗	⊗	≠
Diffusion of carbon during transformation	≠	≠	≠	≠	=	=	=	=
Carbon diffusion controlled growth	≠	≠	≠	≠	=	⊗	⊗	⊗
Cooperative growth of ferrite and cementite	≠	≠	≠	≠	≠	≠	≠	=
High dislocation density	=	=	=	=	⊗	≠	≠	≠
Incomplete reaction phenomenon	≠	=	=	=	≠	≠	≠	≠
Necessarily has a glissile interface	=	=	=	=	=	≠	≠	≠
Always has an orientation within the Bain region	=	=	=	=	=	≠	≠	≠
Grows across austenite grain boundaries	≠	≠	≠	≠	≠	=	=	=
High interface mobility at low temperatures	=	=	=	=	=	≠	≠	≠
Displacive transformation mechanism	=	=	=	=	=	≠	≠	≠
Reconstructive transformation mechanism	≠	≠	≠	≠	≠	=	=	=

Table 2.1 Key characteristics of transformations in steels[from Bhadeshia, 1987, 1992].

Steel[#]:	Pearlite BS11 rail	Pearlite 'D' tyre	Bainite cast M741	Bainite cast VM4059	Bainite cast M740
Code:	**R52**	**W64**	**B04**	**B20**	**B52**
C	0.52	0.64	0.04	0.20	0.52
Si	0.20	0.23	0.19	0.16	0.22
Mn	1.07	0.71	0.80	0.67	0.37
Ni	0.03	0.17	1.93	1.68	1.44
Cr	<0.01	0.18	2.76	2.29	1.70
Mo	<0.01	0.03	0.25	0.27	0.27
S	0.018	0.041	0.009	0.009	0.011
P	0.013	0.023	0.009	0.012	0.013
B	n/a	n/a	0.0023	0.0023	0.0022
Al	n/a	n/a	0.033	0.010	0.028
Ti	n/a	n/a	0.028	0.002	0.028
Cu	n/a	n/a	n/a	0.03	n/a
Sn	n/a	n/a	n/a	<0.01	n/a
B_s°C*	-	-	442	451	442

n/a: not available.

* Bainite B_s temperatures estimated from Haynes amendment[Haynes, 1966] to Stephen and Haynes formula[Stephen and Haynes, 1956] for low carbon bainites:
($B_s \pm 25$°C = 810 - 270C - 90Mn - 37Ni - 70Cr - 83Mo).
Target value 441°C.

R52 was cut from *British Standard 11*[1978] normal grade steel (this standard has since been upgraded in 1985; the rail is similar to UIC 860 grade 70).
W64 was cut from *British Standard 24*[1956], Part 2, Class D tyre (this standard has since been replaced by *British Standard 5892*[1986], Part 4 [10]).
B04, B20 and B52 were experimental casts.

Table 2.2 Composition of steel discs (wt.%)

Mechanical Properties		... Pearlite ...		..... Bainite		
		W64	R52	B04	B20	B52
Hardness	(HV10)	245	220	275	378	355
U.T.S. (P_{max}/A_o)	(MPa)	857	781	924	1235	1321
0.2% proof stress	(MPa)	367	443	638	750	853
Yield stress	(MPa)	325	406	-	-	-
Total plastic elongation	(%)	20.3	21.9	29.8	27.2	12.5
Elongation to necking	(%)	11.7	11.0	4.9	8.4	6.0
Reduction in area	(%)	28.9	35.6	71.9	53.3	22.5
σ_f (* corrected)	(MPa)	1098	1065	1571	1894	1559
σ_u (P_{max}/A_u)	(MPa)	957	867	969	1338	1400
ε_f (ln A_o/A_f)		0.341	0.441	1.268	0.761	0.256
ε_u (ln A_o/A_u or L_u/L_o)		0.110	0.104	0.048	0.080	0.058
ε_n (ln A_u/A_f)		0.231	0.337	1.220	0.680	0.197

* Yamashita's correction for necking [JSME 2 (36) 1966]

σ_f true stress at fracture
σ_u true stress at maximum load, P_{max}
ε_f true strain at fracture
ε_u true strain at maximum load
ε_n true strain from maximum loading to fracture

A_o original cross sectional area
A_f cross sectional area after fracture
A_u cross sectional area at maximum load
L_o original gauge length
L_u gauge length at maximum load

Table 2.3 Mechanical properties of test materials.

Method	Pearlite	..... Bainite		
	R52	B04	B20	B52
Estimated B_s transf. temps. (°C) *		442	451	442
Determined transformation temperatures.				
At Leicester University from cooling curves				air cool / slower cool
Transformation temperature (°C)#	666	493 large 518 small	390	n/d / 401
Cooling rate from 926 - 934°C (Ks^{-1})	1.5	0.7 large 1.1 small	0.6	0.6 / 0.07
Resulant average hardness (HV10)	236	305	413	615 / 441
At British Rail Research (Derby) from dilatometry.				
4 inch section.				
Transformation temperature (°C)	676	513 large 758 small	469	493
Cooling rate from 925 - 926°C (Ks^{-1})	0.5	0.19 large 0.44 small	0.18	0.21
Resultant average hardness (HV10)	240	295	387	525
1 inch section.				
Transformation temperature (°C)	649	493 large	420 large 744 small	241 large 670 small 343 small
Cooling rate from 925 - 926°C (Ks^{-1})	1.48	0.88 large	0.30 large 1.85 small	n/d. large 1.48 small 0.35 small
Resultant average hardness (HV10)	257	307	429	655

The temperatures corresponding to "large" and "small" jumps in the cooling curves, and the corresponding cooling rates, are given.
n/d. Not determined. Air cooling a B52 section at Leicester gave no jump in the cooling curve around the expected Bs temperature; a repeat test with isulated slow cooling did.
W64 was not assessed.

* **Bainite B_s transformation temperatures** estimated from Haynes amendment[Haynes, 1966] to Stephen and Haynes formula[Stephen and Haynes, 1956] for low carbon bainites:
($B_s \pm 25°C$ = 810 - 270C - 90Mn - 37Ni - 70Cr - 83Mo). Target value 441°C.

Table 2.4 Determinations of transformation temperatures.

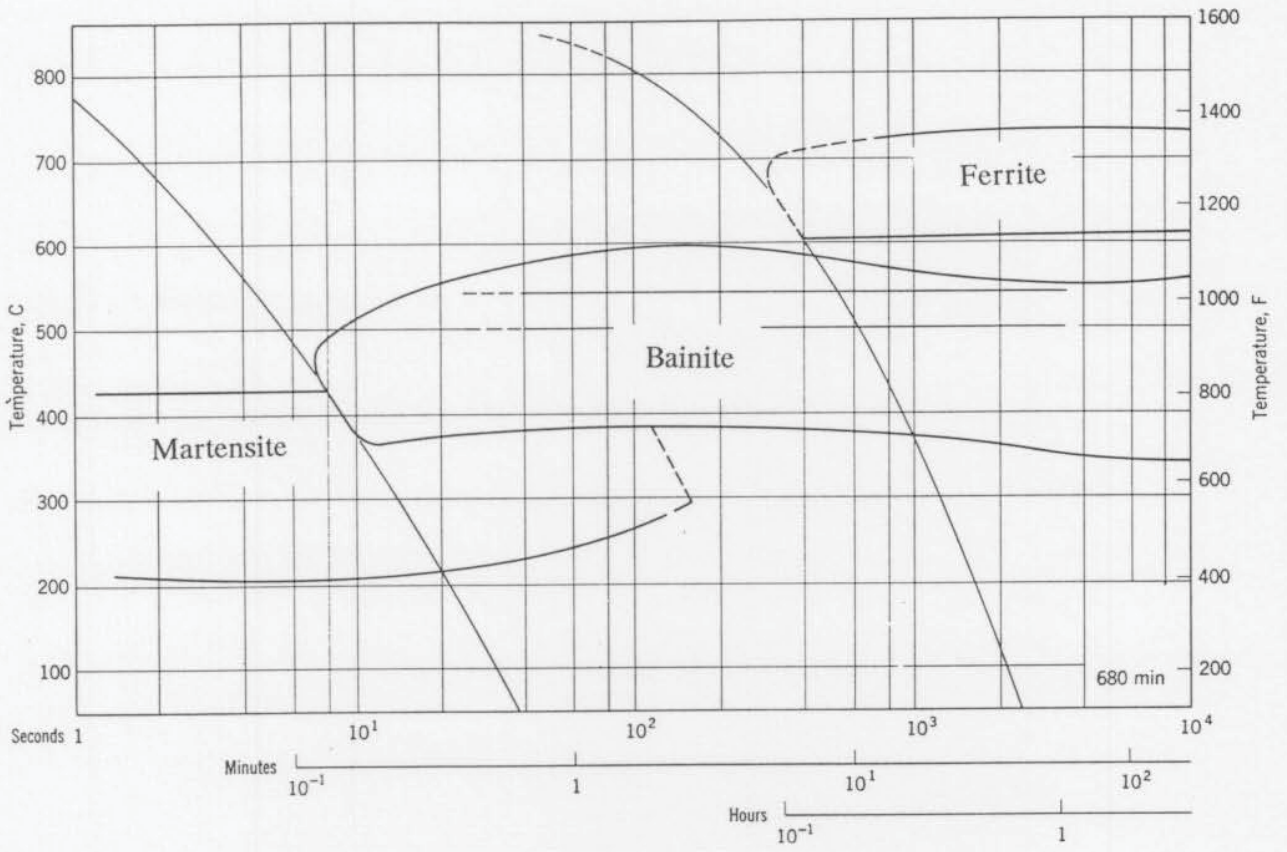

Figure 2.1 CCT diagram of low carbon bainitic structural steel[after Habraken & Economopoulos, 1967]. (Steel composition, wt.%: 0.21 C, 1.46 Mn, 0.38 Si, 0.45 Mo, 0.0017 B, 0.019 S, 0.016 P.)

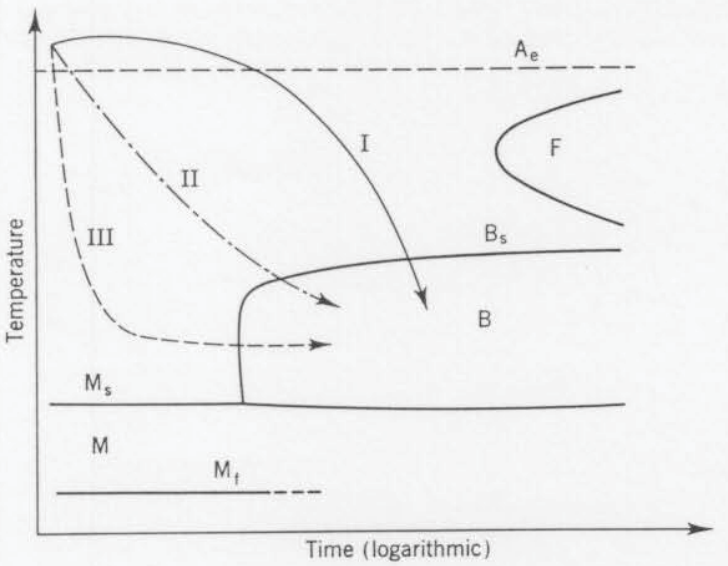

Figure 2.2 Schematic representation of transformation in a low carbon alloy steel[from Habraken and Economopoulos, 1967].

Route 1 produces a structure of ferrite and MA phase particles.
Route 2 produces a carbide free, acicular BI bainite or BII upper bainite.
Route 3 produces BIII lower bainite.

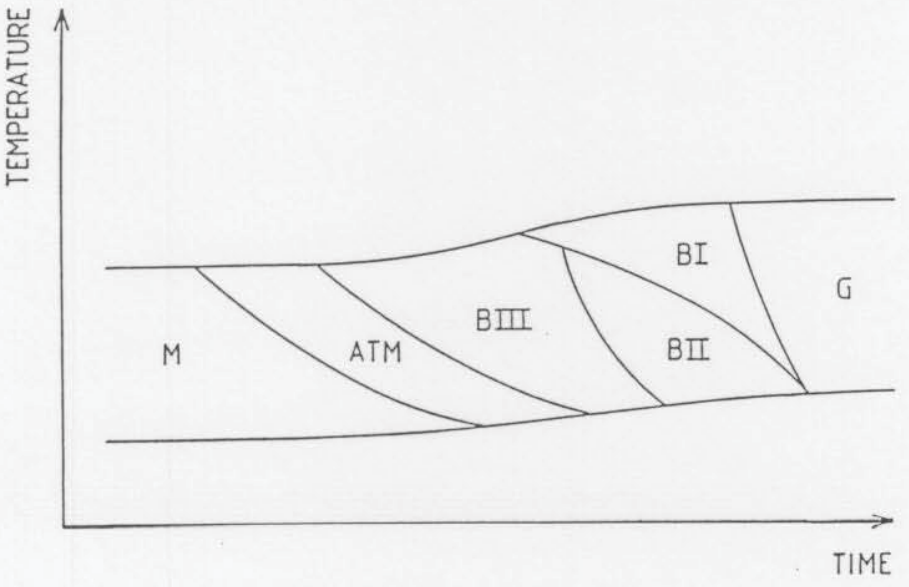

Figure 2.3 Schematic representation of low carbon, low alloy steel structures obtained from different continuous cooling rates[from Callender, 1983].

M	: martensite	ATM	: auto-tempered martensite
BIII	: lower bainite	BII	: upper bainite
BI	: acicular bainite	G	: granular (BIV) bainite.

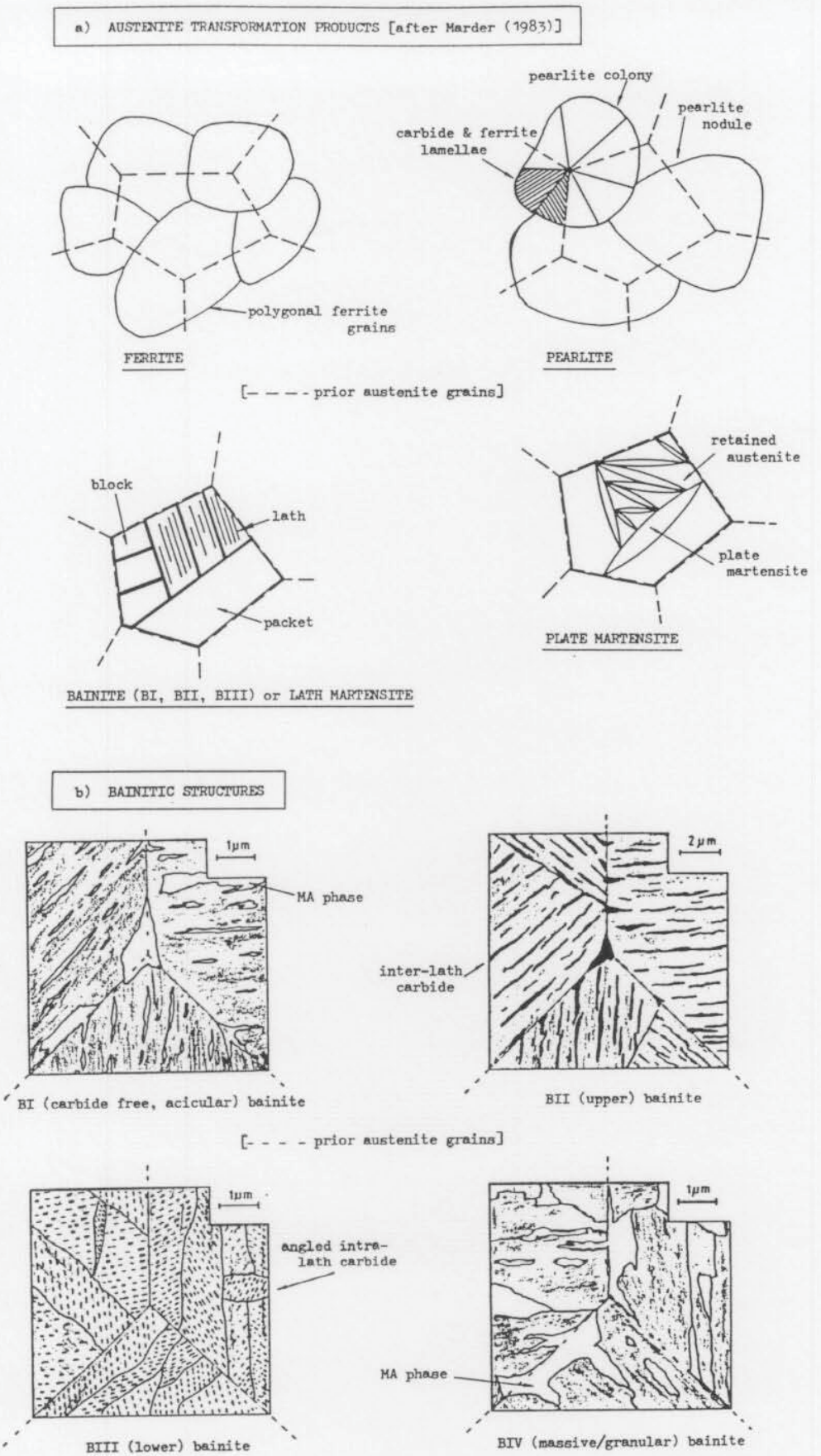

Figure 2.4 Schematic representation of austenite transformation product structures.
(a) A general view of the four types of structure[after Marder, 1983].
(b) The four variations of the steel bainitic structure.

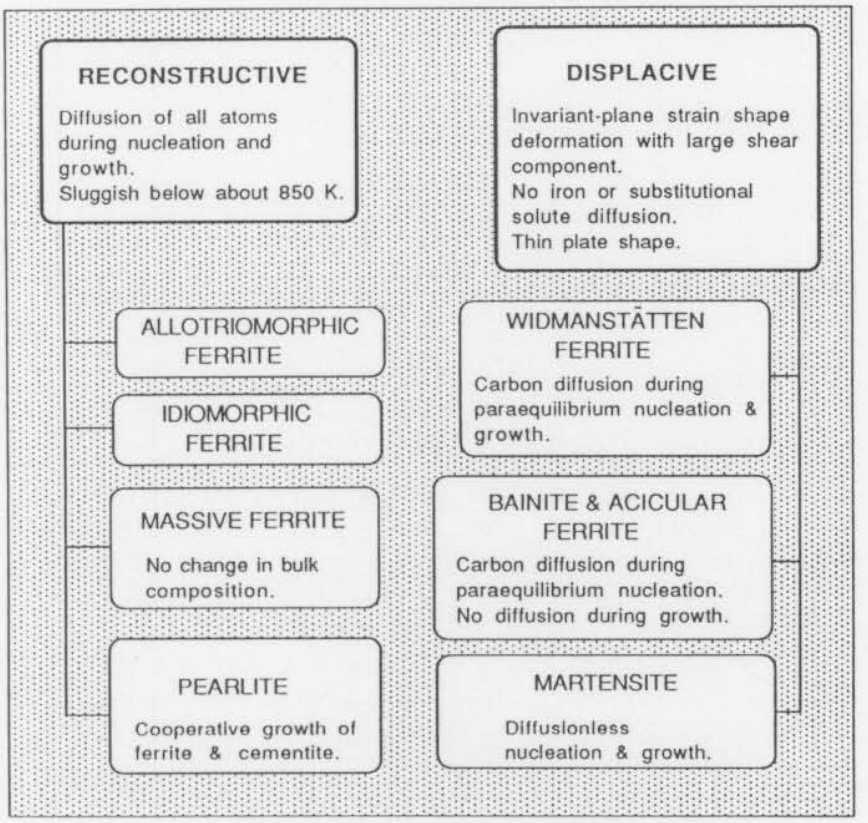

Figure 2.5 Flowchart summarising transformation in steels[from Bhadeshia, 1992].

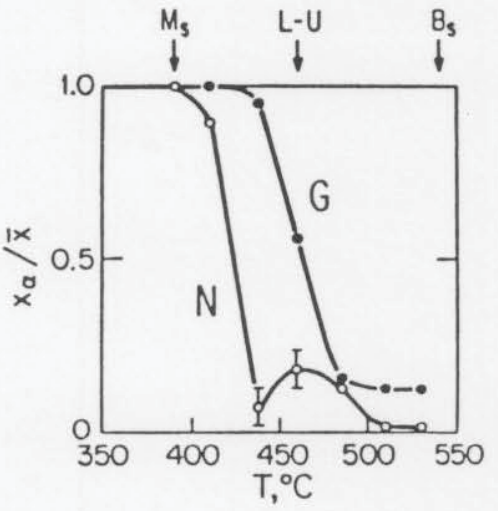

Figure 2.6 Calculated changes in the normalised supersaturation of carbon in ferrite with isothermal transformation temperature for a Fe-0.4C wt% steel[from Olson, Bhadeshia & Cohen, 1987]. ('x_α' is the mole fraction concentration of carbon in ferrite at the austenite-ferrite interface. /x is the average mole fraction concentration of carbon in the alloy. 'G' is the growth curve and 'N' the nucleation curve. 'L-U', lower - upper bainite.)

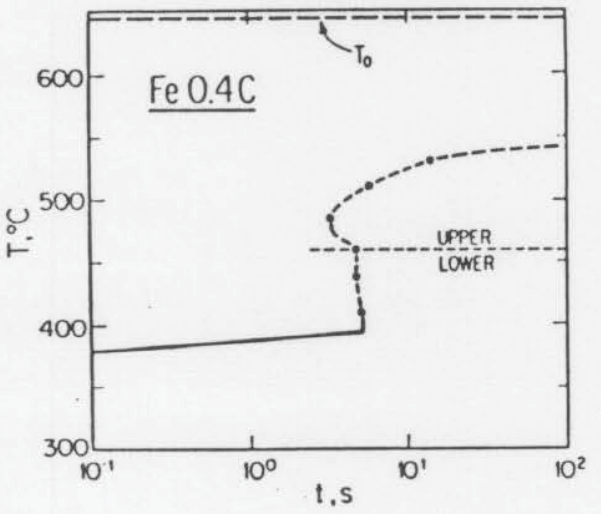

Figure 2.7 Calculated isothermal transformation diagram for a Fe-0.4C wt% steel[from Olson, Bhadeshia & Cohen, 1987].

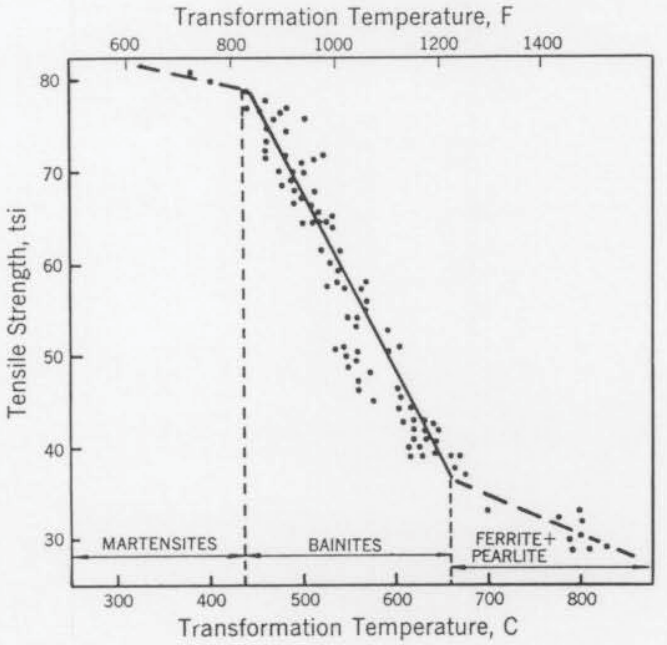

a

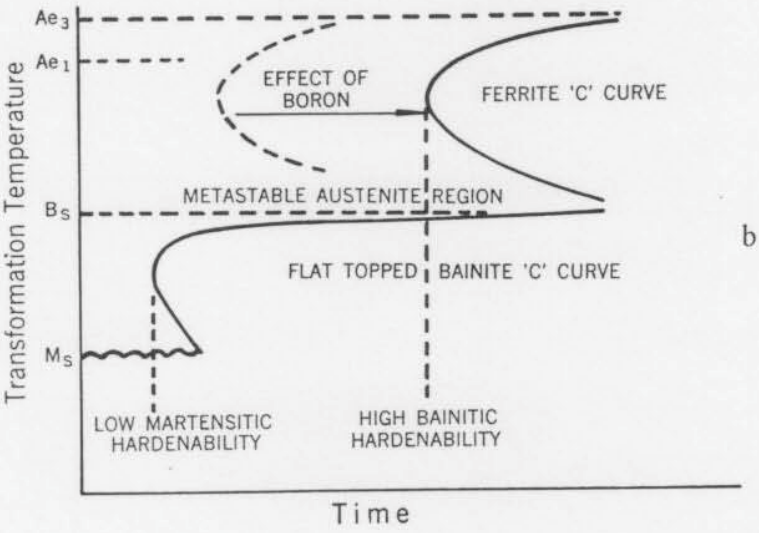

b

Figure 2.8 Transformation characteristics of conventional (upper and lower) bainites[from Pickering, 1967].
(a) Effect of transformation temperature on tensile strength, ranging between that for martensitic and pearlitic structures.
(b) A schematic CCT diagram for a steel which will transform to bainite over a wide range of cooling rates. This is facilitated by the addition of boron to molybdenum steels.

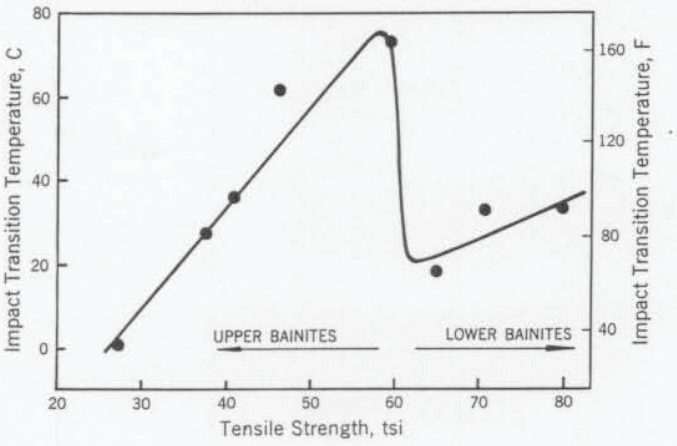

Figure 2.9 Correlation between tensile strength and impact transition temperature for conventional bainitic steels[from Pickering, 1967].

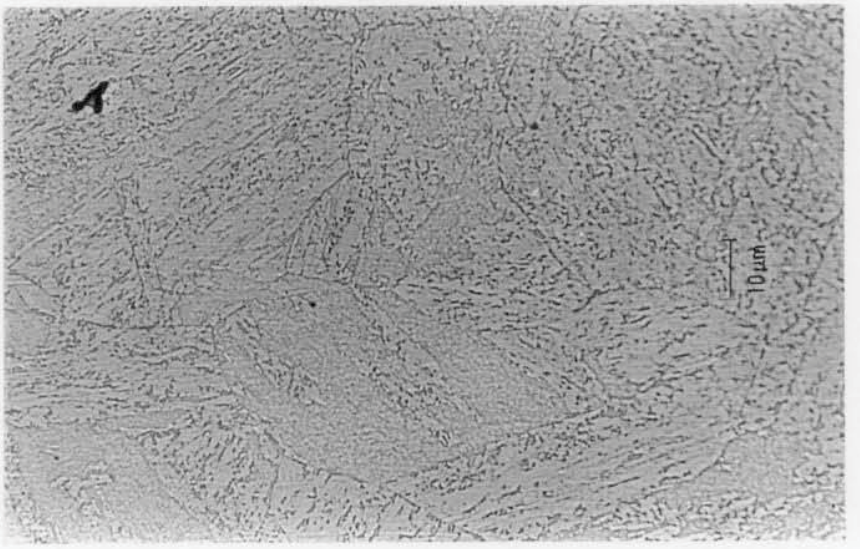

Figure 2.10 Optical micrograph of bainite B04 structure. Barstock transverse section at depth equivalent to LEROS disc surface. Magnification X1000.

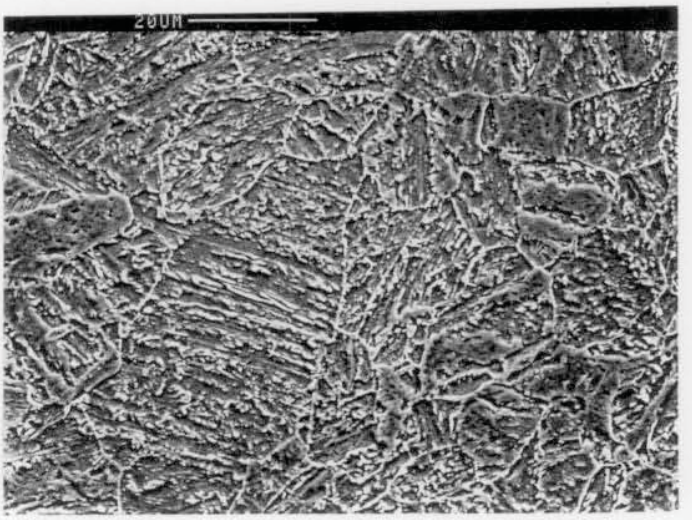

(a) Magnification X1070.

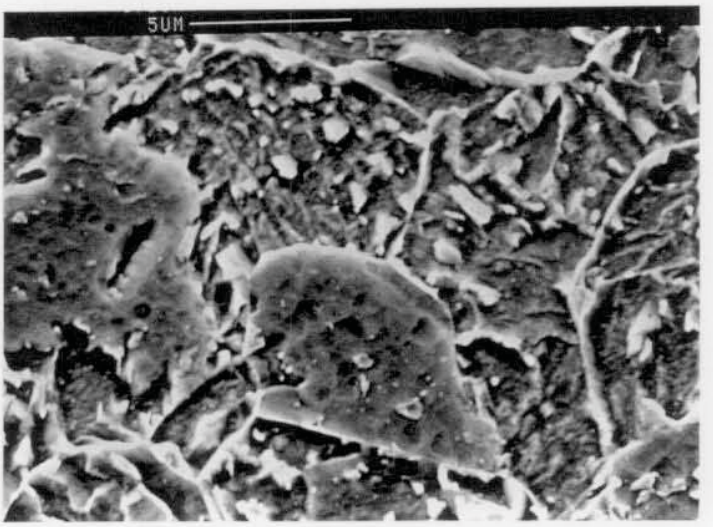

(b) Magnification X5260.

Figure 2.11 Scanning electron micrograph of B04 structure; barstock transverse section at depth equivalent to LEROS disc surface. Dark areas, ferrite, light areas, MA phase.

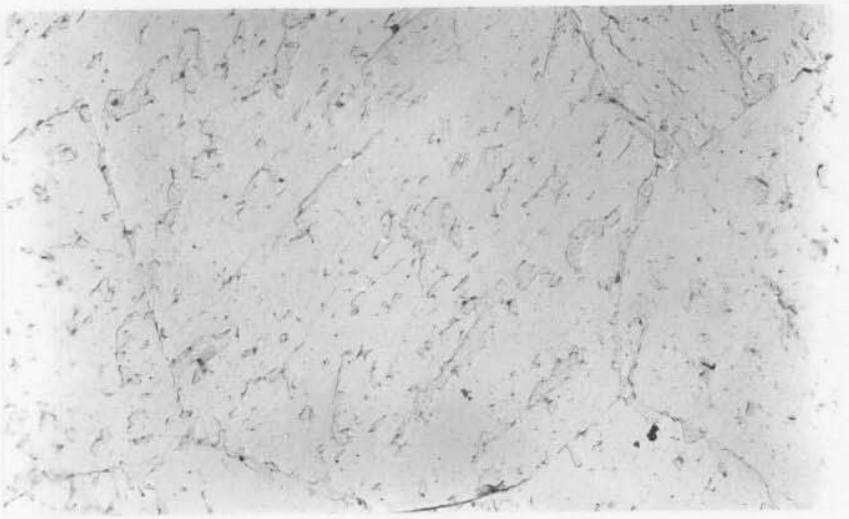

(a) Magnification X3300.

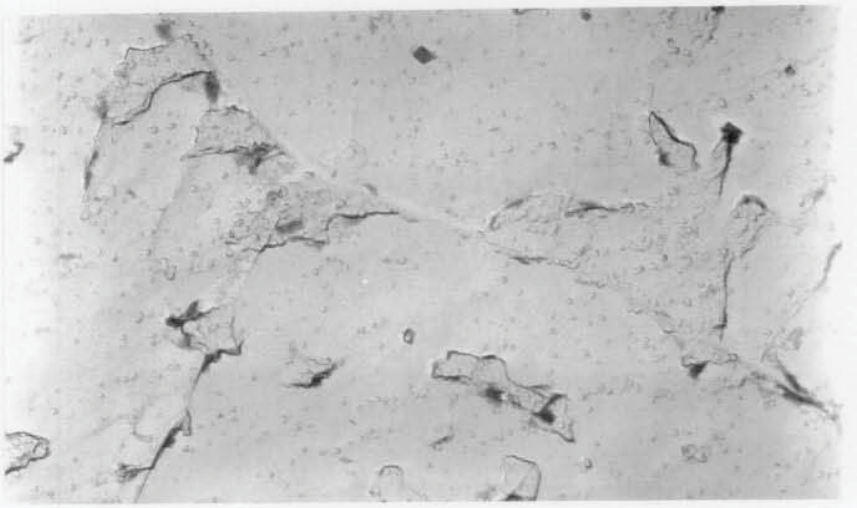

(b) Magnification X20000.

Figure 2.12 Transmission electron, carbon replica micrographs of B04 structure; barstock transverse section at depth equivalent to Amsler disc surface. MA phase at grain boundaries, block boundaries and between laths.

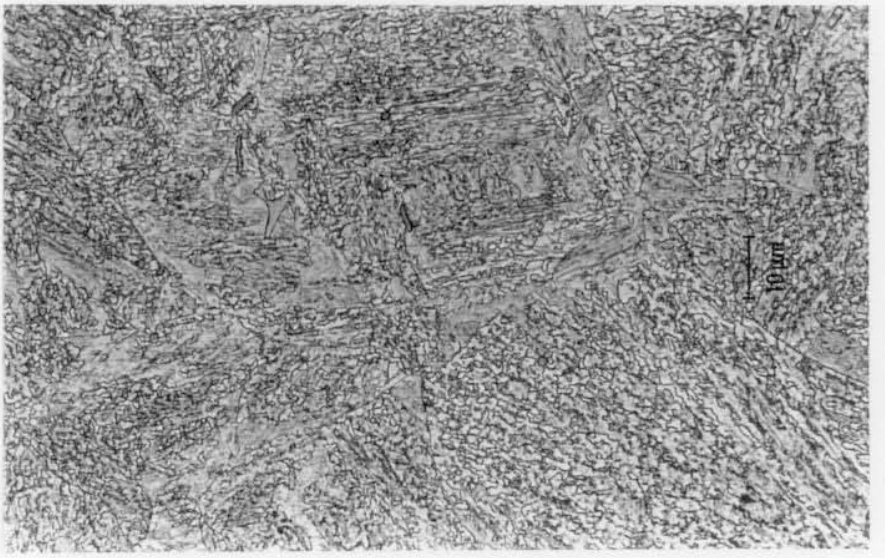

(a) Magnification X1000.

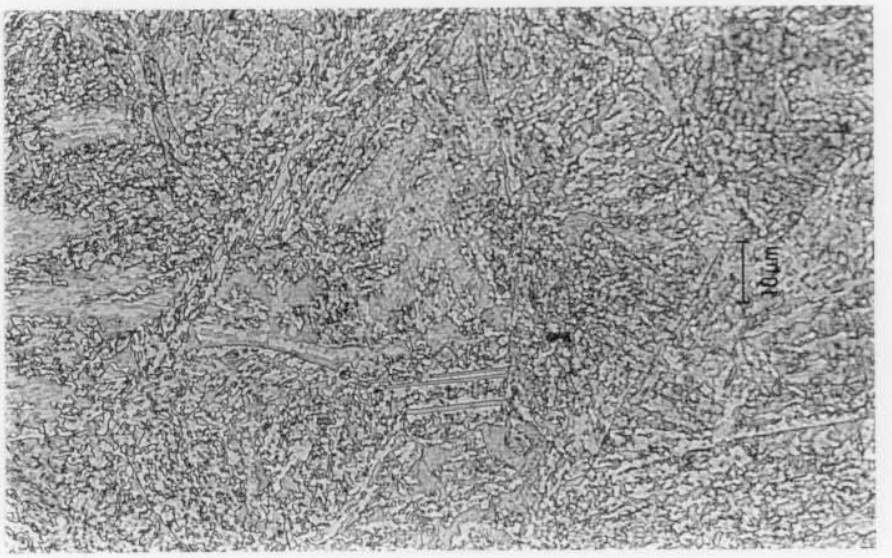

(b) Magnification X1000.

Figure 2.13 Optical micrographs of bainite B20 structure. Barstock transverse section at depth equivalent to LEROS disc surface.
(a) MA phase at grain boundaries. MnS and Ti based inclusions.
(b) Some straight line boundaries typical of massive transformations.

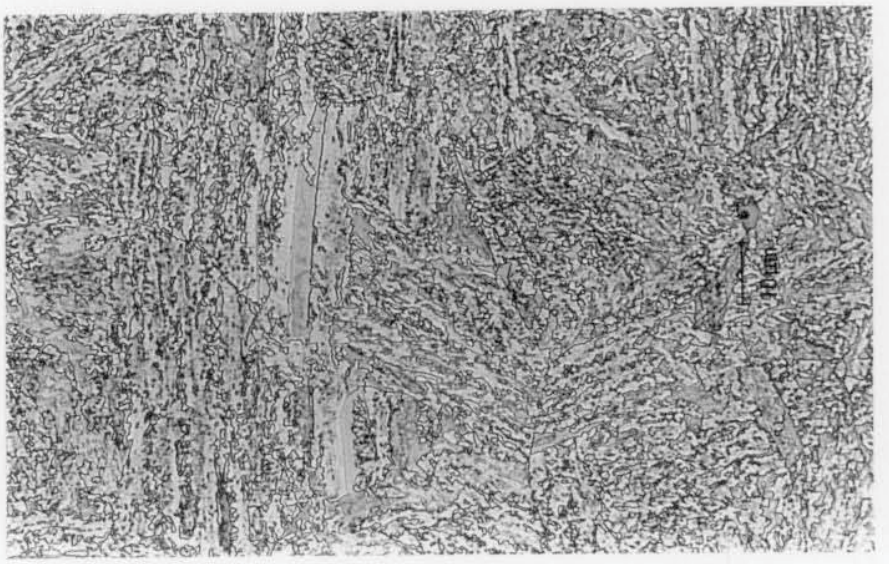

(a) Magnification X1000.

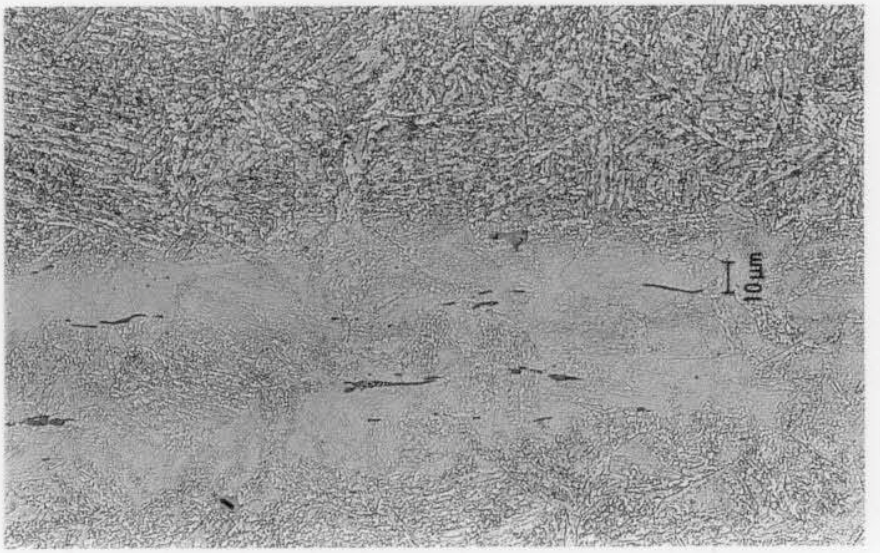

(b) Magnification X500.

Figure 2.14 Optical micrographs of bainite B20 structure. Barstock axial section.
(a) At depth equivalent to LEROS disc surface. Homogenous structure with some straight line boundaries.
(b) Bar centre, Some segregation at this location only, including uneven MnS and Ti based inclusion distributions.

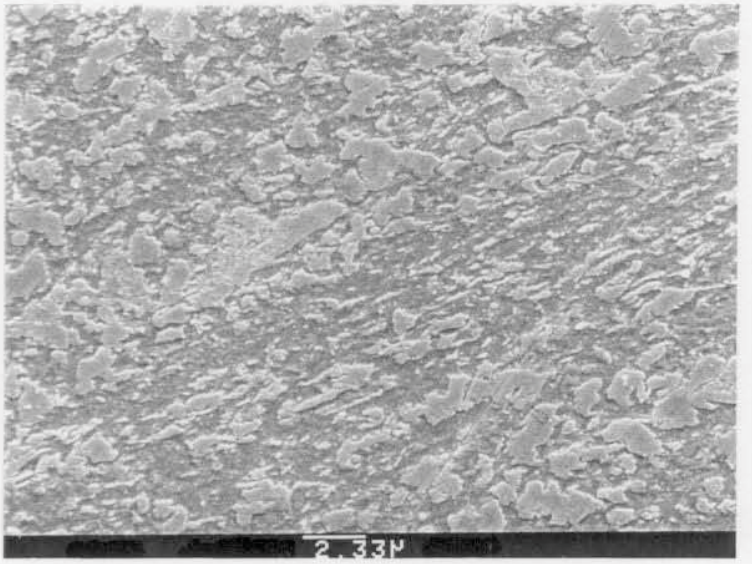

(a) SEM micrograph. Magnification X3700.

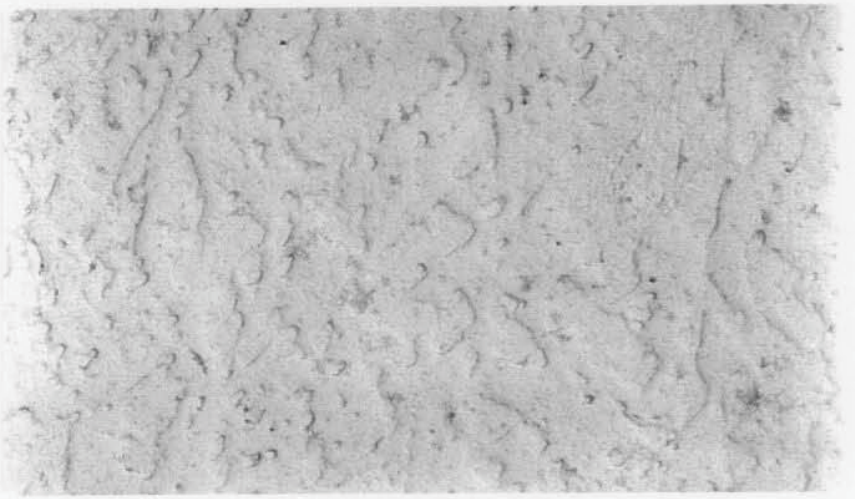

(b) TEM carbon replica micrograph. Magnification X10000, 30° tilt.

Figure 2.15 Electron micrographs of B20 structure. Barstock transverse section at depth equivalent to LEROS disc surface.

(a) Magnification X660.

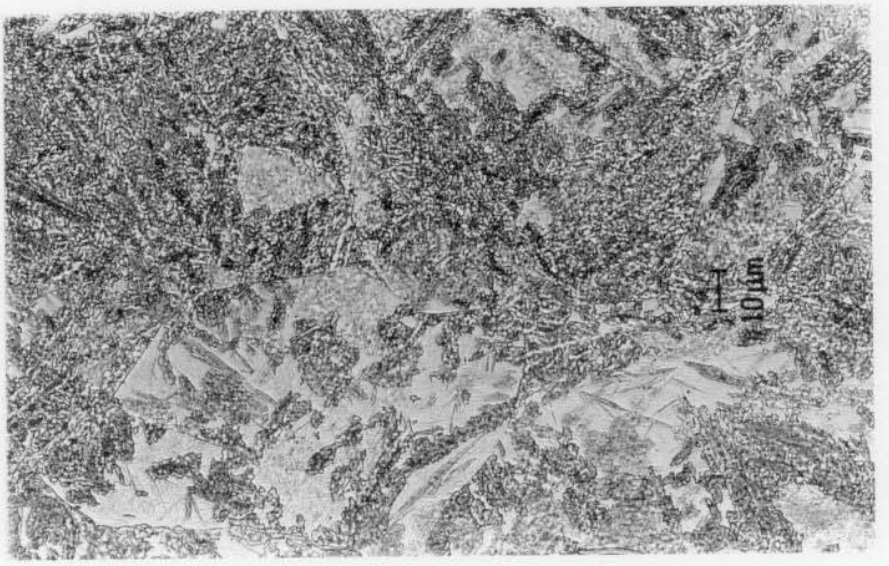

(b) Magnification X660.

Figure 2.16 Optical micrographs of B52 structure. Barstock transverse section at depth equivalent to LEROS disc surface.
(a) Inhomogenous structure - mostly upper bainite with (lighter etching) areas of lower bainite laths in a background of auto-tempered martensite.
(b) The mixed microstructure and clearly delineated prior austenite grain boundaries.

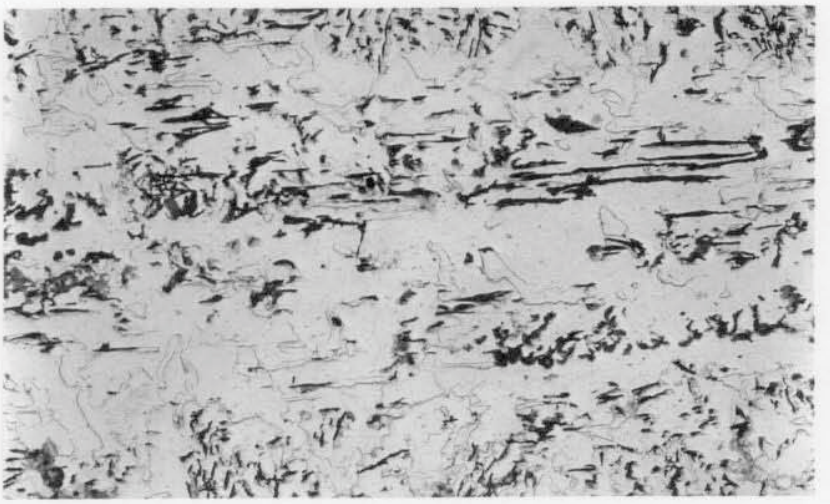

(a) Magnification X5000.

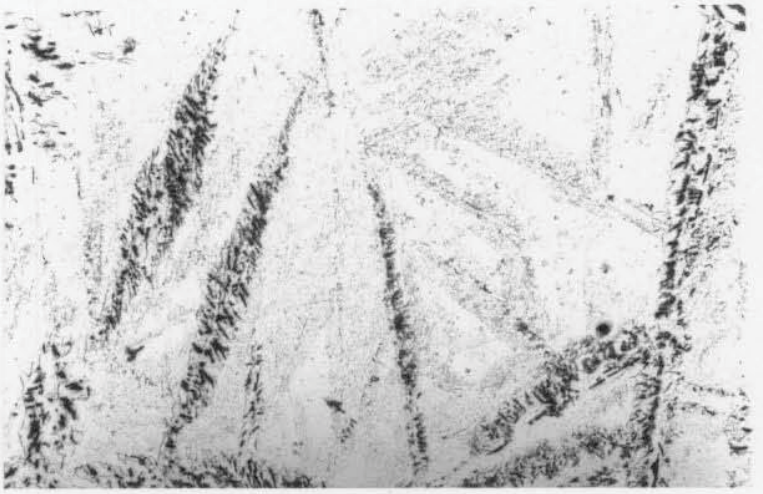

(b) Magnification X7500.

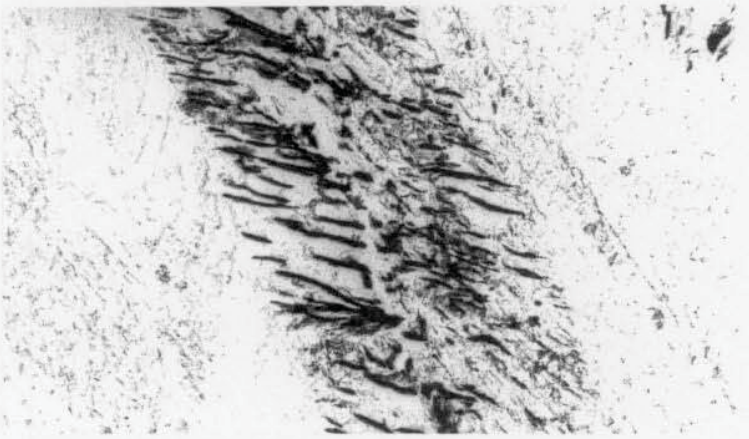

(c) Magnification X22000.

Figure 2.17 Transmission electron, carbon replica micrographs of B52 structure.
Barstock transverse section at depth equivalent to Amsler disc surface.
(a) The upper bainite section of the matrix, showing inter-lath carbide.
(b) The lower bainite / martensite section of the matrix.
(c) Detail of a lower bainite lath showing intra-lath carbide particles angled at 55° to lath axis.

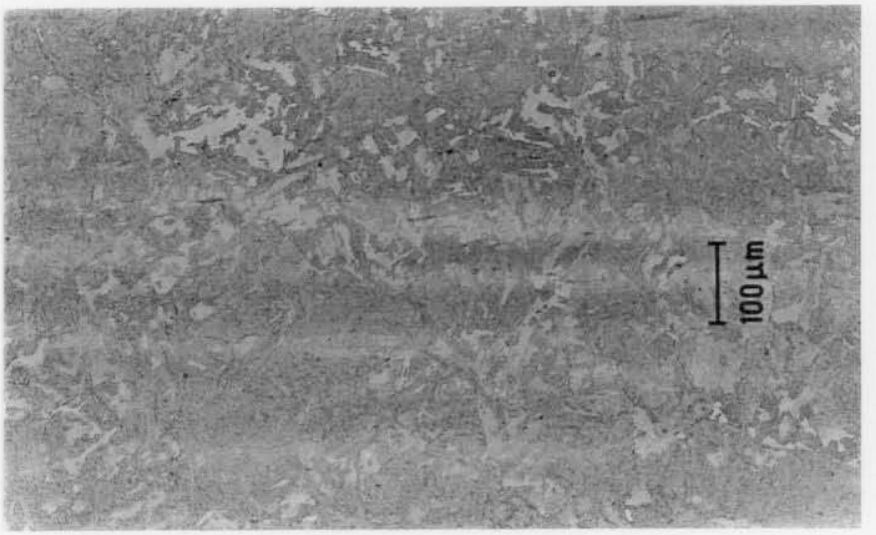

(a) Magnification X112.

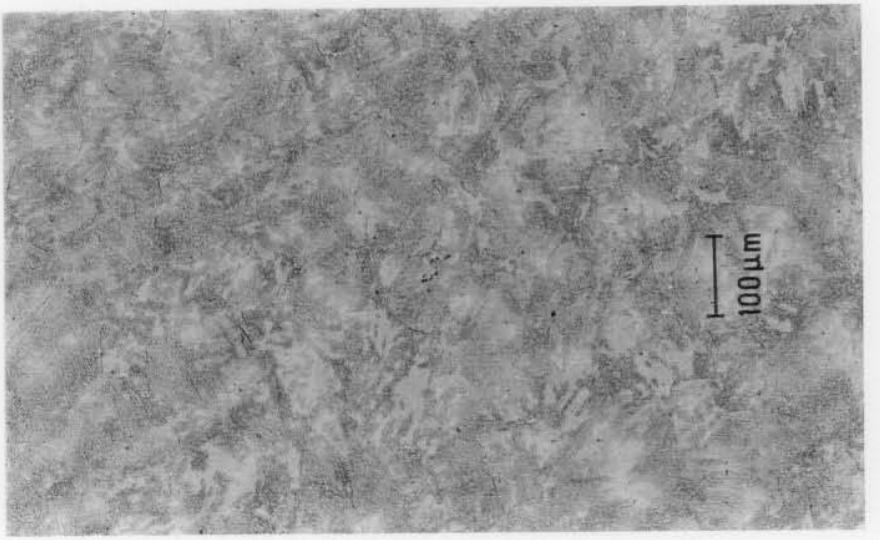

(b) Magnification X112.

Figure 2.18 Optical micrograph of B52 structure. Barstock sections at depth equivalent to LEROS disc surface.
(a) Axial section showing a slight degree of banding.
(b) Transverse section showing distribution of upper and lower bainite regions.

(a) Magnification X200.

(b) Magnification X1000. Note cross-section of MnS stringer.

Figure 2.19 Optical micrograph of R52 pearlitic matrix. Transverse section through rail head at equivalent location to LEROS disc surface.

Magnification X1000. Note typical elongated MnS inclusion.

Figure 2.20 Optical micrograph of W64 pearlitic wheel. Circumferential section from wheel tyre (equivalent to transverse section across disc surface).

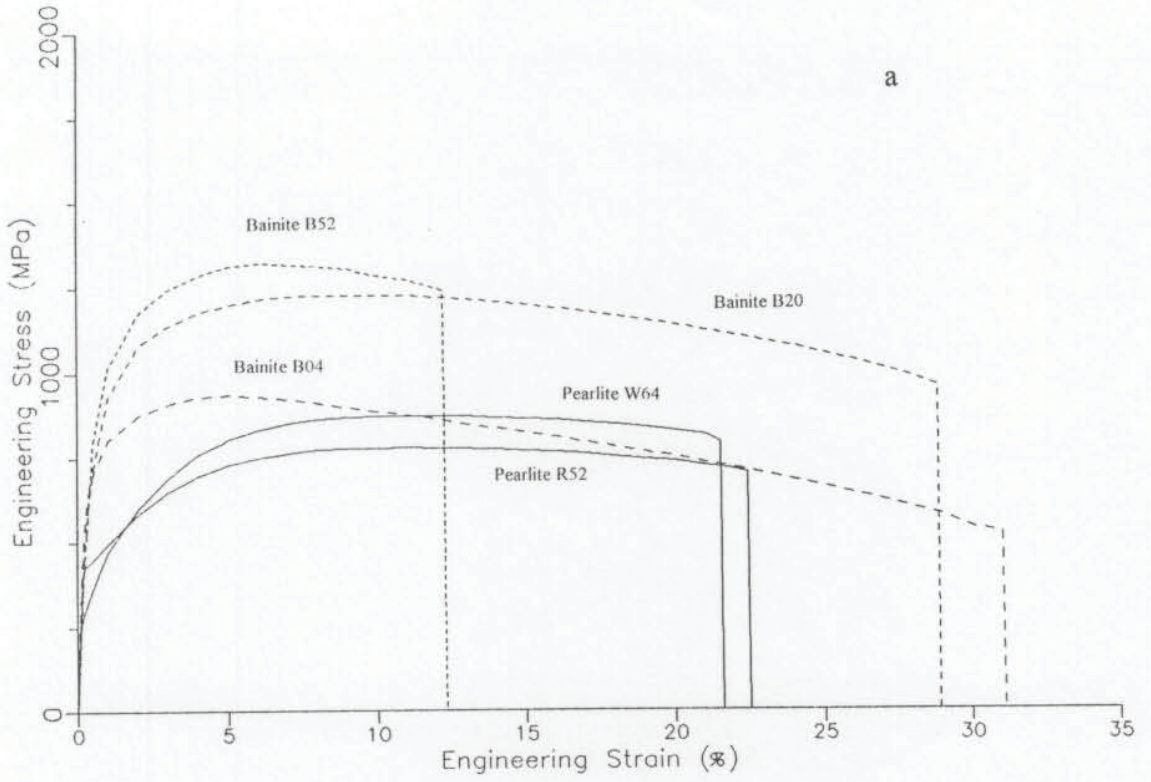

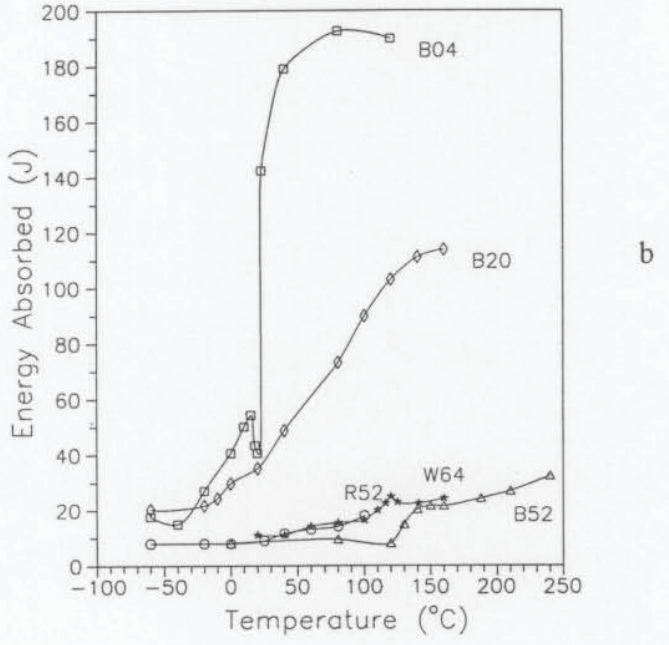

Figure 2.21 Mechanical properties of the experimental steels.
(a) A typical group of engineering stress-strain curves.
(b) Variations in (charpy) ductility with temperature; ductile-brittle transtion temperature curves.

CHAPTER 3

THE CONTACT MECHANICS OF SOLID BODIES SUCH AS WHEEL ON RAIL.

3.1 Nomenclature

A, B, C — Coefficients in equations 3.1 to 3.9.

a — Radius of a circular Hertzian area of contact.

a — Half the contact width of the Hertzian contact strip for cylindrical (line) contact. (This contact can be regarded as a contact ellipse with a major axis "a" of infinite length; i.e., one convention has half the contact width, the ellipse minor axis, as "b". However when considering purely elliptical contact, it is commonly taken as a".)

a, b — Major and minor semi-axes of the contact ellipse of two bodies loaded against each other.

a, b — Half lengths of approximated contact rectangle (cf. Equ. 3.32).

a', b' — Major and minor semi-axes of the elliptical contours of separation of two bodies.

C_{11}, C_{22} etc. — Non dimensional creep coefficients.

c — $c = \sqrt{(ab)}$ where "a and b" are the contact ellipse semi-axes.

D(e), K(e) — Complete integrals of argument, $e = \sqrt{(1-b^2/a^2)}$, $a > b$. (Equations 3.8 to 3.13.)